Journal of Applied Polymer Science

Cell Morphology, Bubbles Migration, and Flexural Properties of Non-Uniform Epoxy Foams Using Chemical Foaming Agent

Lijun Wang,[1] Xu Yang,[2] Tuanhui Jiang,[1] Chun Zhang,[1] Li He[1]
[1]Guizhou Material Industrial Technology Institute, Guiyang, Guizhou 550014, China
[2]The Institute of Materials and Metallurgy of Guizhou University, Guiyang, Guizhou 550003, China
Correspondence to: C. Zhang (E-mail: Zhangchun925@126.com)

ABSTRACT: Epoxy foams with different densities and microstructures were prepared by changing the process parameters including the foaming temperature, chemical foaming agent (CFA) content and precuring extent. The microstructure of foams reveals a smaller cell size, higher cell density, and more homogeneous distribution of cells at higher precuring extent. However, the cell size and distribution are not affected by the foaming temperature and CFA content without precuring process. In addition, the bubbles migration, which resulted in non-uniform cell density distribution, was promoted by increasing the foaming temperature and depressed by increasing the CFA content and precuring extent. The flexural properties of the non-uniform epoxy foams were also studied. Results showed that the flexural modulus was related to the cell morphology, while the flexural strength was affected by both the cell morphology and the position of the specimens during test. It was also found that the relative flexural modulus and strength exhibited a power-law dependence with respect to the relative density. © 2014 Wiley Periodicals, Inc. J. Appl. Polym. Sci. **2014**, *131*, 41175.

KEYWORDS: foams; mechanical properties; morphology; porous materials; thermosets

Received 9 May 2014; accepted 16 June 2014
DOI: 10.1002/app.41175

INTRODUCTION

Epoxy foams have been widely applied to the fabrication of military vehicles, sealant of semiconductor, aircraft, buildings, and so forth due to their excellent properties, including light weight, low moisture absorption, good thermal and chemical stability, and high mechanical properties.[1,2]

In recent years, hollow spherical particles called microspheres have been employed as fillers in epoxy resins. The resultant low-density composites are called epoxy syntactic foams, which are widely studied due to their low weight, high compressive strength, low moisture absorption, and good impact behavior.[3–7] However, this method is difficult to obtain epoxy foams with density below 0.5 g/cm^3 for the limitation of their volume fraction added. Compared with the syntactic foams, it is easy to prepare lower density epoxy foams using a physical or chemical foaming agent. In a physical foaming process, heat causes a low-boiling solvent, such as fluorinert and water, to evaporate thus forming the bubbles.[8–10] For a chemical foaming process, the gas released by the decomposition or reaction of the blowing agent forms bubbles.[2,11–14] These studies are reported in literature only focusing on the cell morphology, process and mechanical properties of the uniform epoxy foams. However, owing to the low viscosity of epoxy mixture, non-uniform dispersed foaming agent, heat dissipation asymmetry, etc, bubbles migration, coalescence and/or collapse in local may take place and then results in non-uniform cell density distribution on a sample, sometimes especially obvious. To date, the non-uniform epoxy foam is studied scare or ignored due to their anisotropic properties such as electric properties.[8,15] This effort is focused on studying the effect of process conditions on the cell structures of epoxy foams and understands how the undesired non-uniform dispersed cell density takes place, though this phenomenon can be avoided by enhancing the viscosity of the epoxy system, for example, a two-step process.[13,14]

It is reported that the mechanical properties of homogeneous epoxy foams are strongly dependent on foam density.[11] Although cell morphology parameters such as cell size, shape, distribution and cell density also have an effect on the mechanical properties at a given density level, their effect can be classified as that of lower importance in comparison with density profile. [11,16–18] On the other hand, the sandwich structural foam, which is a typical non-uniform foamed material, is composed of an unfoamed outer skin surrounding a foamed inner core. The mechanical properties of this foam are affected by the skin thickness, density profile and core ratio.[4,19,20] Thus, the non-uniform cell density distribution, which makes the density difference exist in a specimen, would generate an obvious effect on the mechanical properties. And the present study builds on

Table I. Experimental Conditions of Fabricating Epoxy Foams

Samples	Foaming temperature (°C)	Precuring time (min)	CFA content[a] (wt %)
A	55-65-75-85-95	3	2
B	75	3	0-1-2-3
C	75	3-60-120-150	2

[a] The weight content is based on epoxy matrix.

this knowledge to learn the effects of non-uniform cell density distribution on the flexural properties.

In this study, epoxy foams with different densities and microstructures were prepared by changing the foaming temperature, CFA content, and precuring extent. We investigated the foaming behavior of epoxy foams under different conditions, and especially focused on the non-uniform dispersed cell density. The flexural properties of the non-uniform epoxy foams were studied. And the relationship between the non-uniform foam structures with flexural behavior was also analyzed.

EXPERIMENTAL

Materials

Diglycidyl ether of bisphenol-A epoxy resin (epoxy value = 0.51) and hardener polyamide 650 (amine value = 200–240 mgKOH/g) were supplied by Shanghai Resin Company, China. The chemical foaming agent is p,p-oxybis(benzenesulfonyl hydrazide) (OBSH, molecular weight = 358.39 g/mol), which was supplied by Guangzhou Longsun Technology Company, China.

Sample Preparation

The corresponding amount of CFA was firstly mixed with epoxy resin. To disperse the chemical foaming agent uniformity, the temperature of the mixture was heated up to 60°C and followed by ultrasonication for 10 min. After the mixture cooled down to 35°C, the hardener was added in 100 wt % quantity of the epoxy matrix resin, which was followed by mechanically stirring at 35°C to precure for various time. The slurry then was transferred to preheated stainless steel moulds for foaming. To ensure complete curing, the specimens were maintained at room temperature for 48 h and post-cured at 100°C for additional 2 h.

Three series of foamed samples were prepared by compression molding. Effects of foaming temperature, CFA content and precuring time on the epoxy foams were studied by single factor experiments, and the contents of all formulations studied were summarized in Table I.

Characterization

Morphology of Foams. Microstructures of the epoxy foams were characterized by scanning electron microscope (SEM, KYKY-2800B, China). The fractured surfaces were coated with gold for SEM observation. The SEM pictures were analyzed by the software Image Pro. With this method, the cell density (N_f) was determined by the number of cells per unit volume of foam, which was calculated using eq. (1)[21,22]:

$$N_f = \left(\frac{nM^2}{A}\right)^{3/2}\left(\frac{1}{1-V_f}\right) \quad (1)$$

where V_f is the void fraction; n, M and A are the number of cells in the micrograph, the magnification of the micrograph, and the area of the micrograph (cm^2), respectively. The V_f was determined using the following equation:

$$V_f = 1 - \frac{\rho_f}{\rho_m} \quad (2)$$

where the densities of unfoamed (ρ_m) and foamed (ρ_f) samples were obtained according to the Archimedes principle.

The average cell diameter (D) was calculated using eq. (3):

$$D = \frac{\sum d_i n_i}{\sum n_i} \quad (3)$$

where n_i is the number of cells with an area-equivalent diameter of d_i.

Mechanical Properties. Flexural tests according to ISO 178 standard were made in a universal testing machine (Shenzhen SANA, China) using three-point bending mode with a 64 mm span. At least five specimens were tested. Specimen dimensions for flexural testing were 80 mm × 10 mm × 5 mm. And a load rate of 2 mm/min was maintained for testing. Flexural modulus was determined from the slope of the initial portion of the flexural stress–strain curve. Flexural strength (σ_f) was calculated using the equation:

$$\sigma_f = \frac{3PL}{2bh^2} \quad (4)$$

where P is the maximum load, L is the span length; b and h are the breadth and thickness of the specimen, respectively.

RESULTS AND DISCUSSION

Morphology of Epoxy Foams

Effects of Foaming Temperature on Epoxy Foams. Figure 1 shows the SEM images of specimens foamed at different temperatures. It can be observed that the cells were discrete with a closed-cell structure, nearly spherical and surround by thick walls. The cell morphology parameters of epoxy foams, such as average diameter, cell density, and cell size distribution, are shown in Figure 1(f) and Table II. The width of the cell size distribution peak, which represents the dispersity of the cell size, was little affected by the foaming temperature. From Table II, it can be seen that the mean cell size was about 300 μm at the range of foaming temperature from 55°C to 95°C, while the cell density almost increased by five times.

Noteworthy, the uniformity of the foamed material was obviously affected by the foaming temperature (Figure 1). The whole fracture surface of the non-uniform foams can be categorized into three layers, namely, (i) the upper layer where the cell density is the highest, (ii) the middle layer means transition layer and (iii) the under layer where the cell density is the least. The cell density of the upper layer was higher than that of the under layer (Figure 2), and the thickness of the upper loose layer increased with the increasing foaming temperature. It means that the bubbles migrate from the bottom up and then

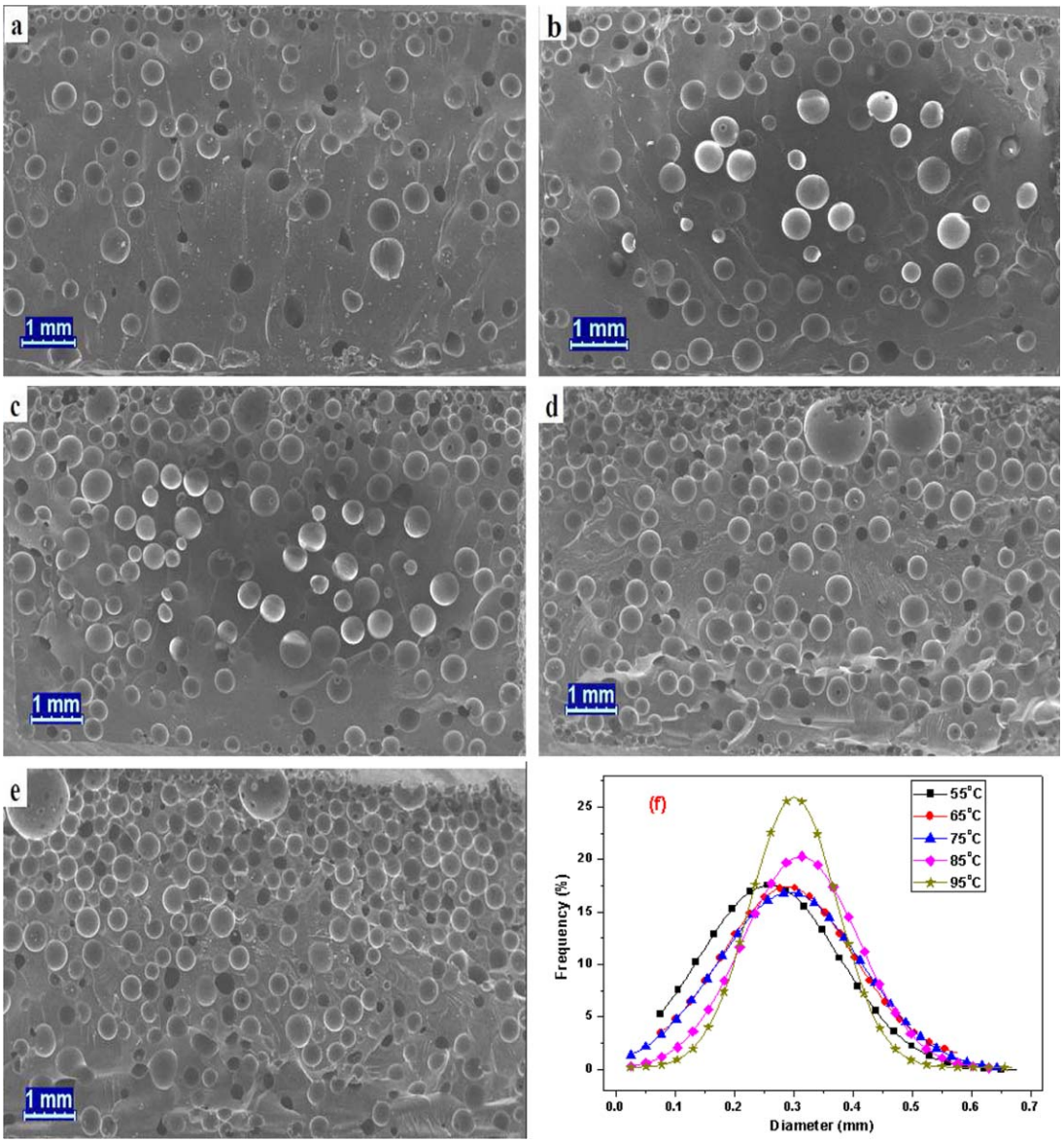

Figure 1. SEM micrographs for epoxy foams produced at different foaming temperatures: (a) 55°C; (b) 65°C; (c) 75°C; (d) 85°C; (e) 95°C; and (f) cell size distribution. [Color figure can be viewed in the online issue, which is available at wileyonlinelibrary.com.]

stack from top to bottom, which is similar to the Stacking Blocks game. On the other hand, the bubbles at the top would collapse to form large bubbles and even ruptured duo to the interfacial tension and low pressure at the top, leaving behind some vacancies and then these vacancies would be filled up again by bubbles migrated from the next layer. With the intensification of the curing process, the viscosity of system increased dramatically, the cells were solidified gradually, and namely the migration process was over. This migration can be the reason why the cell density decreased from top to bottom on the whole cross-section. Furthermore, it is clear that the thickness of the upper layer is dependent on the bubbles stacking process and bubbles eliminating process (collapsed and ruptured). A higher foaming temperature generates a lower initial viscosity and higher blowing pressure related to decomposing of CFA,[23,24] which promotes the bubbles migration and thus results in a thicker upper layer. However, bubbles coalescence and collapse become drastic, especially above 75°C, which makes the bubbles on upper surface display an open-cell structure as shown in

Table II. Cell Morphology Parameters and Density of Epoxy Foams Produced at Different Temperatures

Foaming temperature (°C)	Diameter (μm)	Cell density (cells/cm^3)	Density (g/cm^3)
55	280	5.900×10^3	0.900
65	300	8.251×10^3	0.846
75	300	1.890×10^4	0.711
85	320	2.002×10^4	0.695
95	310	3.114×10^4	0.624

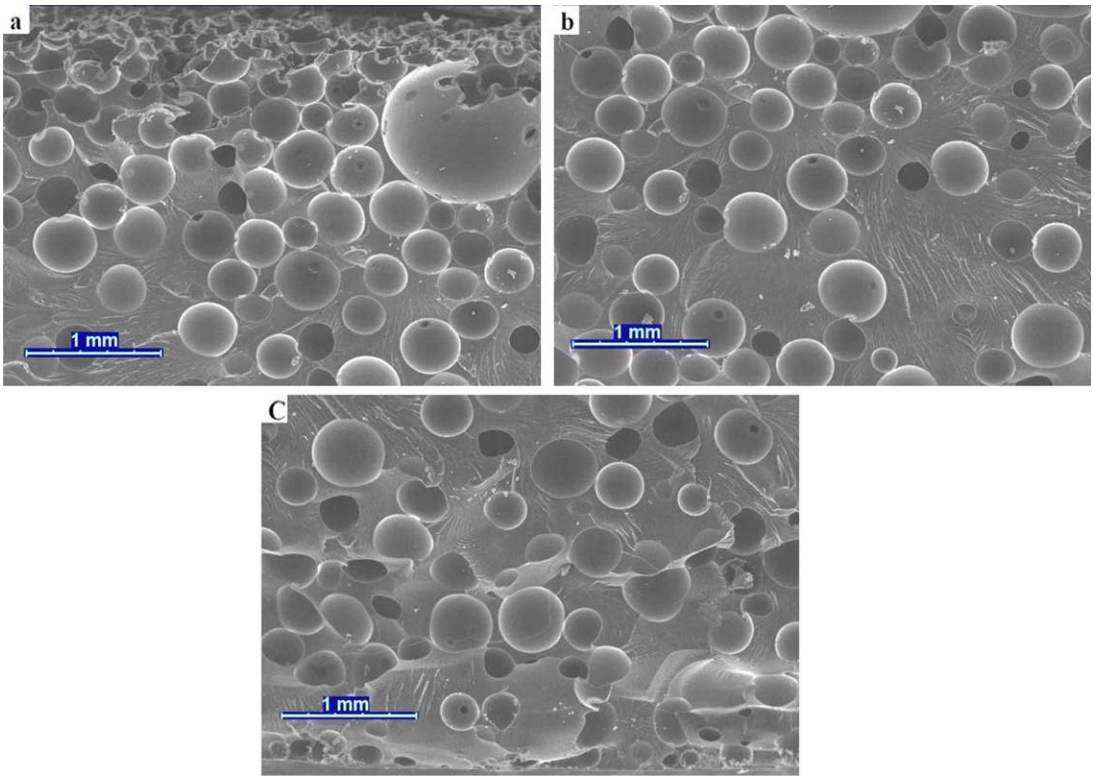

Figure 2. SEM micrographs for epoxy foams produced at 85°C: (a) upper layer; (b) middle layer; (c) under layer. [Color figure can be viewed in the online issue, which is available at wileyonlinelibrary.com.]

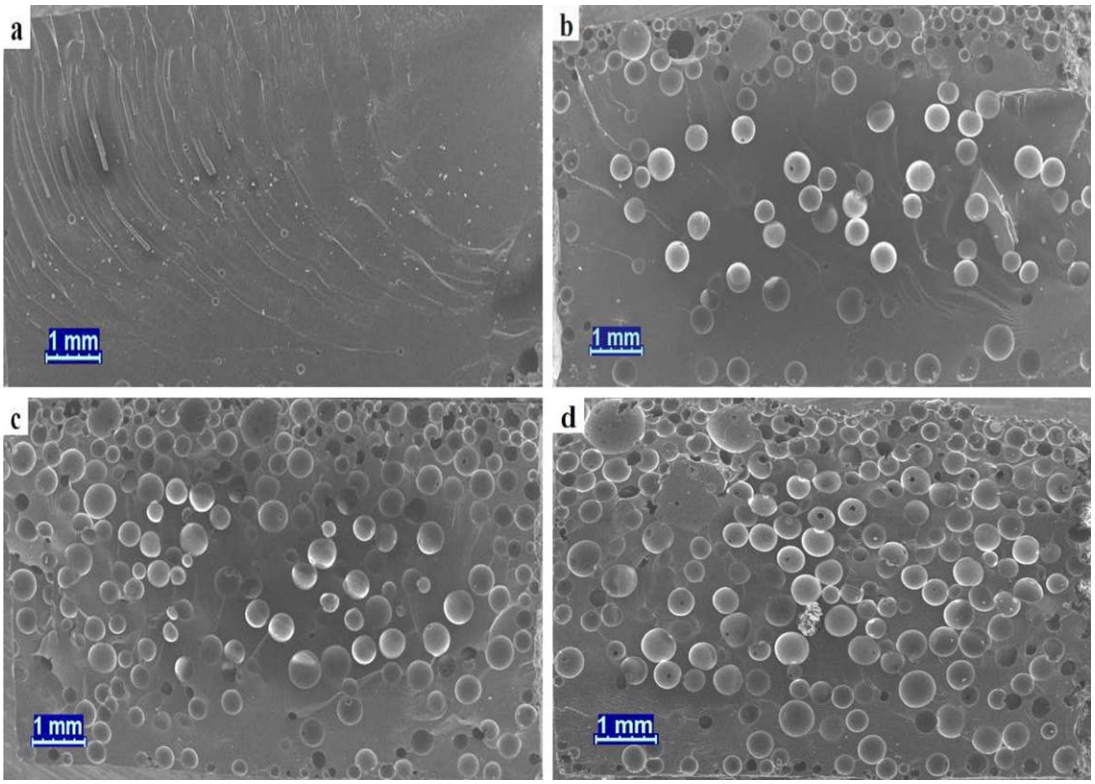

Figure 3. SEM micrographs of the foamed samples using different CFA content: (a) 0%; (b) 1%; (c) 2%; (d) 3%. [Color figure can be viewed in the online issue, which is available at wileyonlinelibrary.com.]

Table III. Cell Morphology Parameters and Density of Epoxy Foams Using Different CFA Content

CFA content (wt %)	Diameter (μm)	Cell density (cells/cm^3)	Density (g/cm^3)
0	-	-	1.055
1	300	6.726×10^3	0.874
2	300	1.890×10^4	0.711
3	310	2.121×10^4	0.648

Figure 2(a). On the other hand, as the foaming temperature increases, the curing reaction rate of epoxy mixture increases, leading to the quick increasing viscosity and short gel time, which is advantage for bubble stabilization. As a result, the non-uniform epoxy foams with closed-cell structure were obtained at high foaming temperature, excepting the upper surface above 75°C. On contrary, at low temperature, bubbles migration is limited by high initial viscosity. However, there is enough time for bubbles growth due to low curing reaction rate.[25] As a result, the homogeneous foamed material with large cell size was obtained [Figure 1(a)].

Effects of CFA Content on Epoxy Foams. Figure 3 shows the effect of CFA content on the cell morphology of samples foamed at 75°C without precuring process. The corresponding cell morphology parameters of epoxy foams are shown in Table III and Figure 4. It was found that the cell density increased with increasing the CFA content, while the cell size and distribution remained unchanged at the experimental range. The change in cell size followed with CFA content is different from other reports,[11,22,24] which claimed the average diameter decreased when the CFA content decreased. The different results here could be due to the low viscosity of epoxy mixture in this study. The bubbles migration phenomenon, which resulted in non-uniform material, was also observed in all foams [Figure 3(b–d)]. In addition, as the CFA content increased, the thickness of the upper loose layer increased and the boundary between upper layer and middle layer was gradual indistinct.

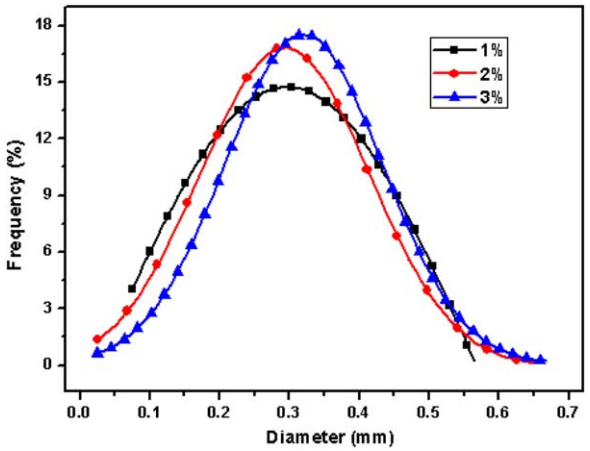

Figure 4. Effect of CFA content on the cell size distribution of epoxy foams. [Color figure can be viewed in the online issue, which is available at wileyonlinelibrary.com.]

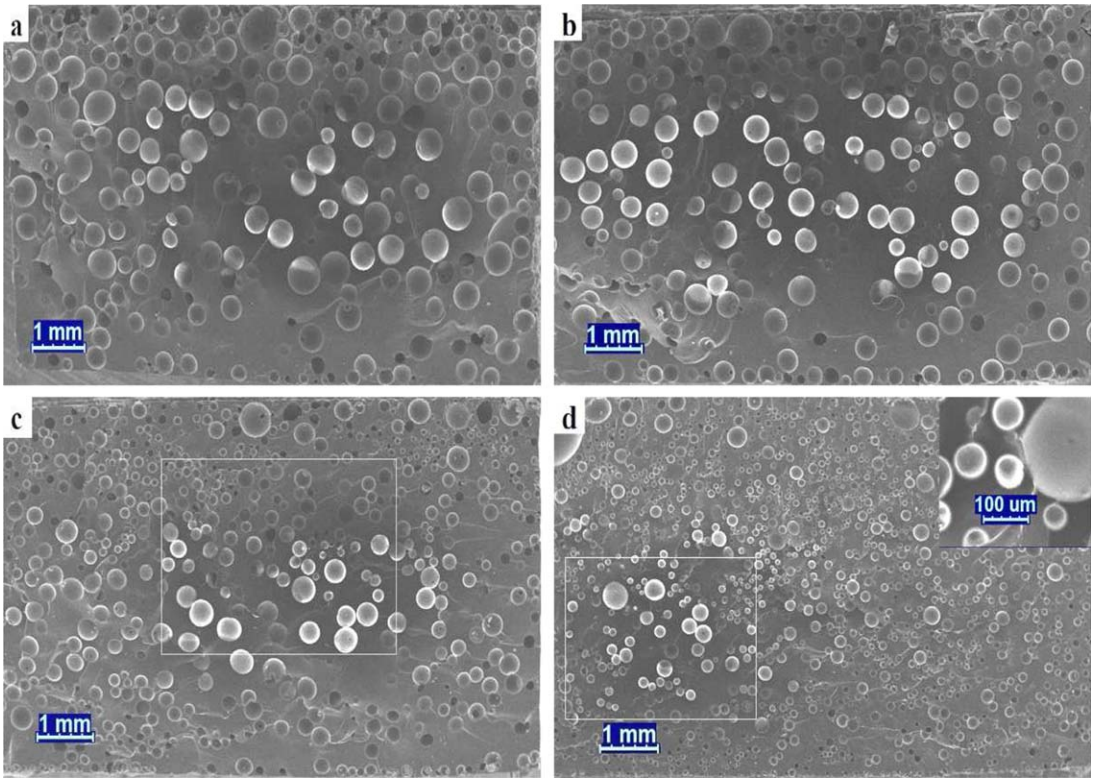

Figure 5. SEM micrographs of the foamed samples with different precuring extent: (a) 89 Pa·s; (b) 102 Pa·s; (c) 165 Pa·s; (d) 397 Pa·s. [Color figure can be viewed in the online issue, which is available at wileyonlinelibrary.com.]

Table IV. Cell Morphology Parameters and Density of Epoxy Foams with Different Precuring Extent

Viscosity (Pa·s)	Diameter (μm)	Cell density (cells/cm^3)	Density (g/cm^3)
89	300	1.890×10^4	0.711
102	290	1.757×10^4	0.758
165	180	4.906×10^4	0.806
397	105	2.255×10^5	0.858

This can be explained by that a higher CFA content generates more gas for cell nucleation and growth,[22] and then more bubbles would migrate to upper layer, which results in increased upper layer at the same foaming temperature.

Effects of Precuring Extent on Epoxy Foams. Epoxy mixture with 2% CFA content was precured at 35°C for different time and then foamed at 75°C to obtain the epoxy foams. The effect of precuring extent on the cellular structures of epoxy foams is illustrated in Figure 5. The viscosity at 35°C, measured by rotary viscosimeter (NDJ-1B, China), is used to describe the precuring extent. Table IV and Figure 6 shows the viscosity-dependence, namely precuring extent-dependence, of the foam structural parameters. With the increase of the precuring extent, the average cell diameter decreased whereas the cell density increased, and the width of the cell size distribution peak decreased, which indicated that the uniformity of the cell size got better at relatively high precuring extent. This is because epoxy mixture with high precuring extent has high viscosity and short gel time.[13,25] The enhanced viscosity, which prevents further expansion of the bubbles, would reduce the average cell diameter. The short gel time, which shortens the bubbles growth process, would make the size distribution uniformity. However, although the precuring time is long up to 150 min, the foam is still composed of big bubbles with small bubbles around them as shown in Figure 5(d). This phenomenon was also confirmed by other reports[2,11,13,14] and the explanation was given by Keping Chen.[14] However, the bimodal size distribution is not obvious at this study. What is more, the uniformity of the cell density distribution seems to get better as the precuring extent increases, though the bubbles are not dispersed uniformly on the whole cross-section for all the foams. For Figure 5(a) and (b), the cell density decreased from top to bottom can be easily understood for the bubbles migration from the bottom up as description above. However, the cell density distribution in Figure 5(c) and (d) was different from that. As shown in Figure 5(c), the relative large bubbles with a low cell density existed in the middle layer, around which relative small and dense bubbles dispersed. High magnification SEM micrograph in Figure 7(a) clearly presents this structure [rectangular box in Figure 5(c)]. In addition, the cell density in the upper layer of the cross-section was also higher than that of bottom layer. At the initial foaming process, the bubbles migrated from the bottom up slowed down at high precuring extent due to the enhanced viscosity. With the intensification of the curing process, the viscosity of system further increased, and the heat produced by curing of epoxy and decomposing of CFA was accumulated and hard to dissipate in the middle layer of the sample, which caused higher local temperature. The bubbles in this local would further grow, coalesce to form large bubbles, and then resulted in an expansion force which would make lots of bubbles around this place. Further increasing the precuring extent, the growth process of bubbles in the high temperature local was hindered and shortened, which resulted in forming discrete and small local with relative large bubbles and low cell density as shown in Figure 5(d) (rectangular box). And this high magnification SEM micrograph is shown in Figure 7(b). Furthermore, the gradient distribution of cell density can be also seen at this precuring extent [Figure 7(d)]. A wide middle layer with dense bubbles and under layer with the least bubbles can be observed in the high magnification SEM micrographs [Figure 7(d), right]. This is due to the bubbles migration from the bottom up but without enough time. As a result, at high precuring extent, the cell density distribution on the whole cross-section is ascribed to the two different ways of bubbles migration, namely whole migration and local migration.

Flexural Properties

The density of the foams as a function of temperature is represented in Table II. The density decreased from 0.900 g/cm^3 at 55°C to 0.624 g/cm^3 at 95°C. Similar to the density, the flexural properties exhibit the same trend as shown in Figure 8(a). It can be found that the flexural properties of these foams decreased with the increasing foaming temperature. Epoxy foams exhibited strength of 42.95 MPa and modulus of 1207.47 MPa at 55°C in contrast to the strength of 14.38 or 16.62 MPa and modulus of 431.28 MPa at 95°C for the same weight fraction of CFA. Interestingly, when the foaming temperature is above 75°C, the flexural strength is related to the location of the samples. The flexural strength is higher when the compact layer (lower cell density) is far away from the load cell. However, the flexural modulus is not affected by the location. Figure 8(b) and (c) shows the effect of CFA content and precuring extent on the flexural properties, respectively. The flexural strength and modulus decreased with the increasing CFA content, while increased with increase of the precuring extent. In

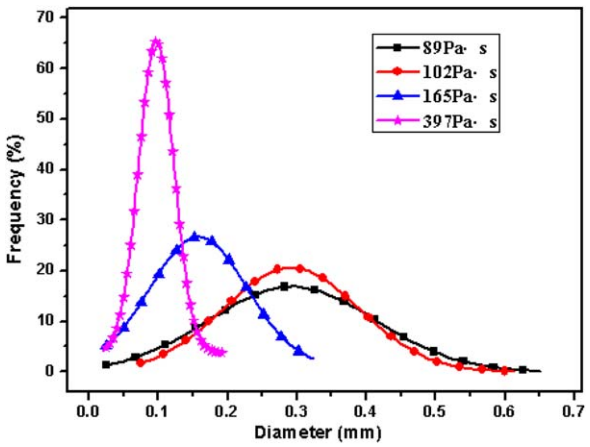

Figure 6. Effect of precuring extent on the cell size distribution of epoxy foams. [Color figure can be viewed in the online issue, which is available at wileyonlinelibrary.com.]

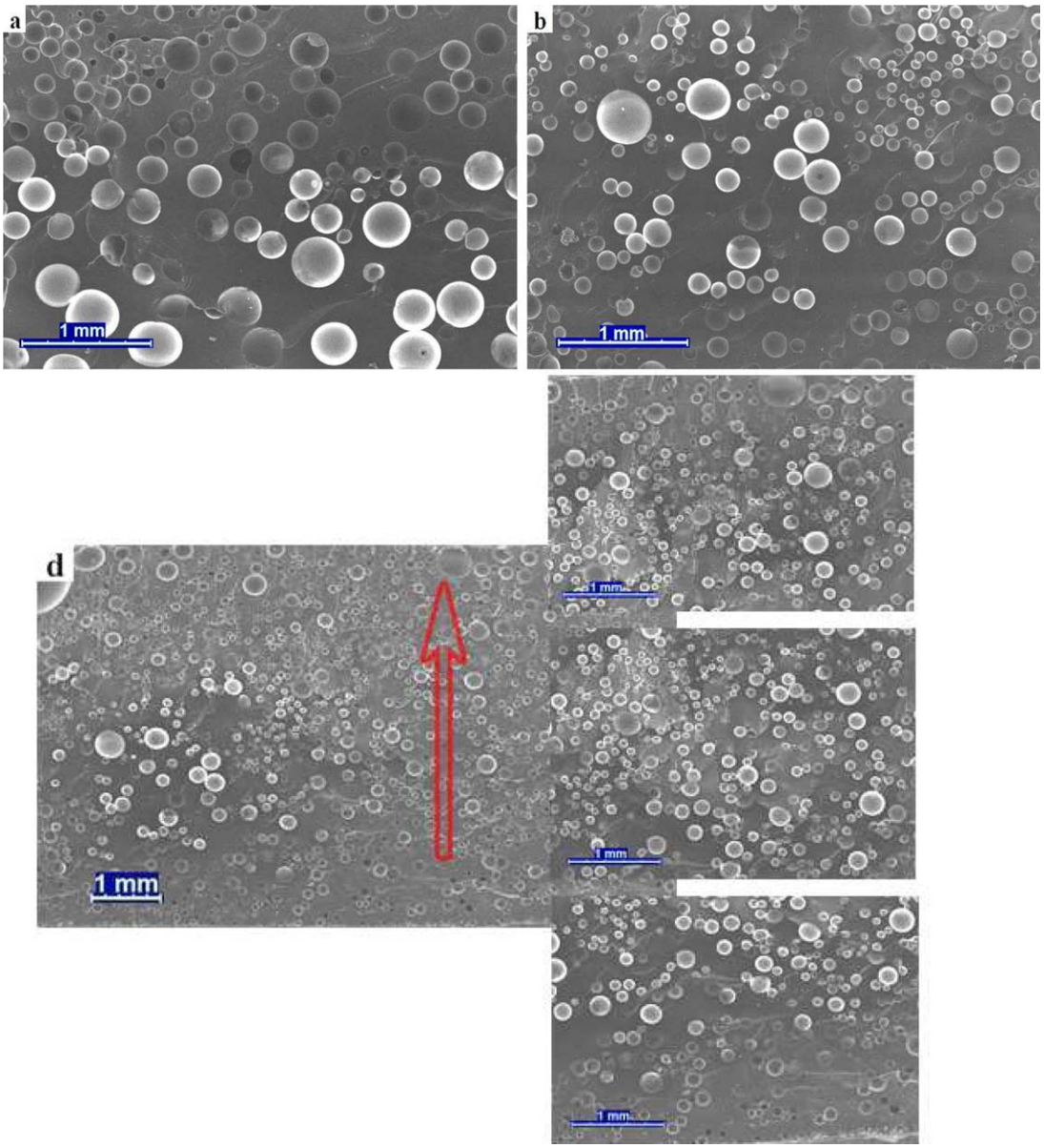

Figure 7. High SEM micrographs of the foamed samples with different precuring extent: (a) 165 Pa·s; (b, d) 397 Pa·s. [Color figure can be viewed in the online issue, which is available at wileyonlinelibrary.com.]

addition, as the viscosity (precuring extent) increased, the flexural properties increased quickly first and then slowed down. This is due to the better cell morphology at higher precuring extent as shown in Figure 5. But whatever, the flexural modulus and strength of foamed epoxy composite cannot surpass that of the unfoamed composite (1577.23 MPa and 54.26 MPa, respectively).

Currently, the simple theoretical model used to predict the mechanical properties of closed-cell polymer foams is developed by the generalized mixture rule. For a foamed product, it can be considered as a two-phase composite with negligible mechanical properties of the dispersed phase. As a result, the mechanical properties of polymer foams are generally related to their density by the formula.[11,16–18]

$$\frac{M_f}{M_m} = A\left(\frac{\rho_f}{\rho_m}\right)^n \quad (5)$$

where M is any specific property such as Young's modulus, yield strength, compressive modulus, etc. ρ is the density and subscripts f and m represent the foamed and unfoamed matrix, respectively. A is a constant related to the physical properties of the resin, and n is the density exponent related to the structure and deformation mechanics of cellular material.[11,18,26] Over the range of density analyzed, a good fit of flexural modulus and strength is obtained for values of density.

In order to further investigate the effect of foaming temperature, CFA content and precuring extent on the flexural properties of epoxy foams, the M_f /M_m as a function of ρ_f/ρ_m under different conditions is shown in Figure 9. From Figure 9(a), it can be

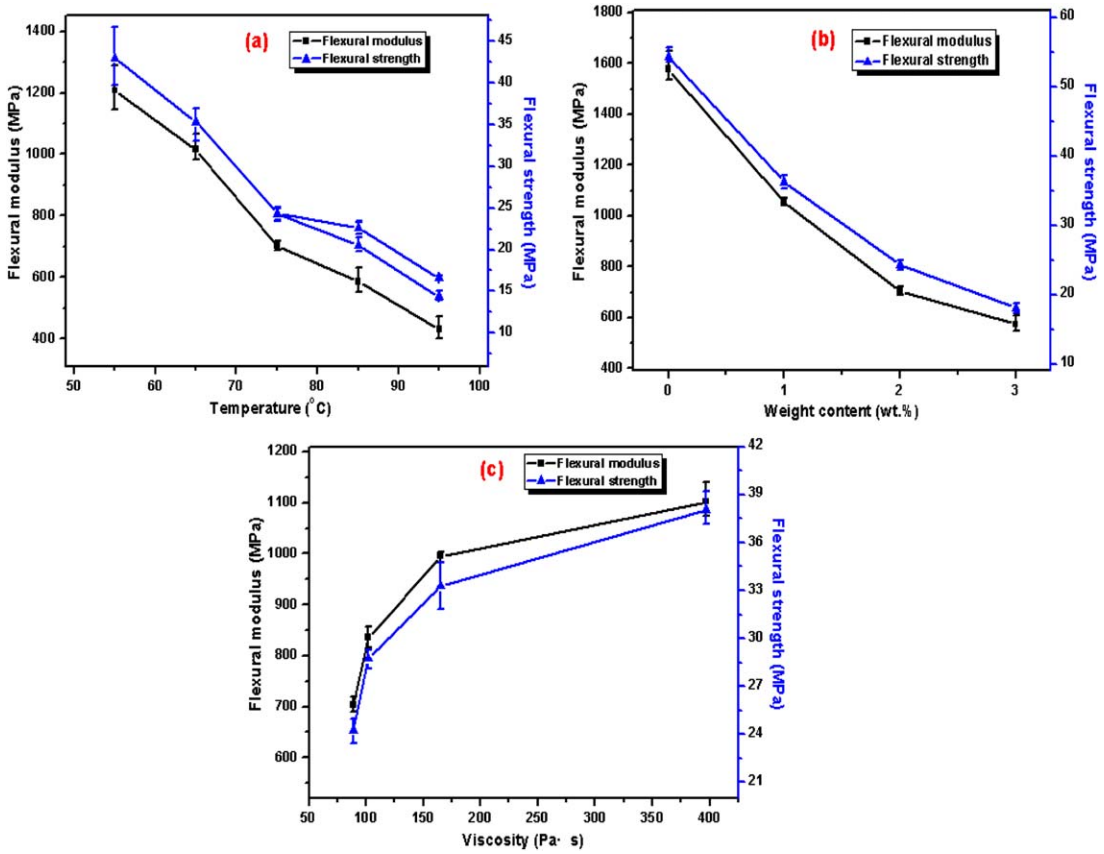

Figure 8. The effect of (a) foaming temperature, (b) CFA content, and (c) precuring extent on the flexural properties of epoxy foams. [Color figure can be viewed in the online issue, which is available at wileyonlinelibrary.com.]

found that, in lower relative density (ρ_f/ρ_m), epoxy foams exhibit higher relative flexural modulus (E_f/E_m) under CFA content variable compared with foaming temperature variable but the contrary in higher relative density. As above description, the epoxy foams prepared by changing the foaming temperature and the CFA content showed nearly the same average cell diameter and cell size distribution. In low relative density, the cell density under CFA content variable dispersed more uniform than that under foaming temperature variable, which differs from in high relative density. As a result, the difference between foaming temperature and CFA content variables in E_f/E_m of epoxy foam is ascribed to the effects of uniformity of the cell density. That is, non-uniform cell density, which makes the material non-uniform, would result in low flexural modulus. In addition, the E_f/E_m for precuring extent variable exhibited the highest values at a given relative density level. This is because the precuring extent variable produces an obvious improvement in the cell morphology compared with the foaming temperature and CFA content variables, and thus

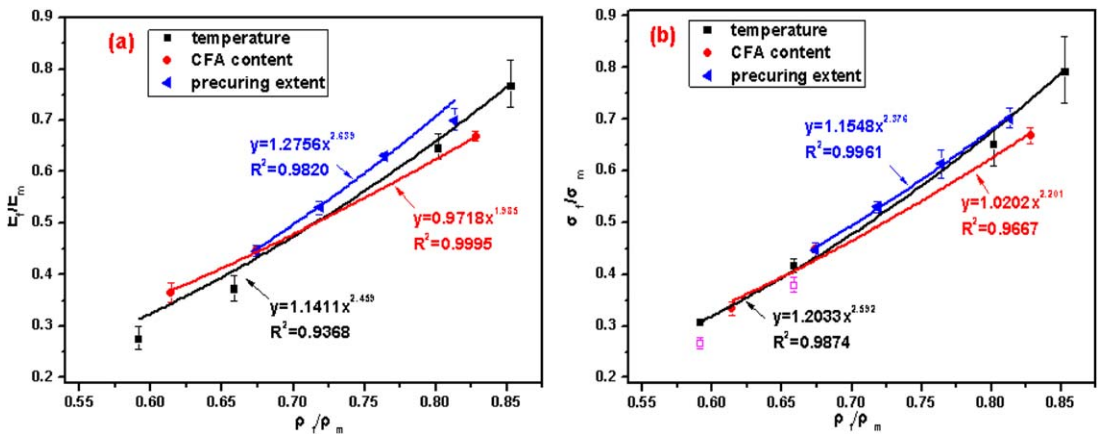

Figure 9. Relative density dependence of the relative flexural modulus (a) and strength (b) in flexure. [Color figure can be viewed in the online issue, which is available at wileyonlinelibrary.com.]

enhances the flexural modulus the most. The relative flexural strength (σ_f/σ_m) with respect to the relative density (ρ_f/ρ_m) under different processing conditions, including foaming temperature, CFA content and precuring extent, is represented in Figure 9(b). Unlike the relative flexural modulus, there is no obvious difference in the three fitting curves. It means that the flexural strength of epoxy foams is significantly affected by the apparent density but not the uniformity of the cell density. Note that, there are two hollow dots in this figure, which are downward departure from the curves. These values were obtained when the loose layer (high cell density) of the non-uniform specimen was far away from the load cell, which were lower than those when the loose layer was near to the load cell. This is because the failure process of foamed samples initiates first in the tensile side of the specimen during flexure and is followed by a sudden and catastrophic failure.[4,5,27–29] For the non-uniform foam material, when the loose layer is far from the load cell under tensile stresses, the specimen will fail at lower strength due to the high cell density and open-cell structure on surface as show in Figure 2.

Further study will focus on the failure mechanism of the non-uniform epoxy foams under different flexural strain rates. And the effect of location of the foams during test on the flexural properties will be further investigated to clarify the critical value of the non-uniform cell density distribution.

CONCLUSIONS

Epoxy foams with different densities and microstructures were prepared. The effect of process parameters including the foaming temperature, CFA content and precuring extent on density, microstructure and flexural property of composites were investigated. The following are the conclusions of the present study:

1. The cell size and distribution are not affected by the foaming temperature and CFA content without precuring process, while the cell density increases with increasing both of them. The decreased cell density distribution from top to bottom on the whole cross-section is due to the bubbles migration from the bottom up.
2. The microstructure of foams reveals a smaller cell size, higher cell density, and more homogeneous distribution of cells at higher precuring extent. However, the non-uniform cell density distribution, which is ascribed to the whole and local bubbles migration, is also observed at high precuring extent.
3. Whatever the process parameters are, the relative strength and modulus of the non-uniform foam exhibits a power-law dependence on the relative density. The flexural modulus of the foam is affected by the cell density distribution, while the flexural strength is not sensitive to that. When the bubbles on upper surface exhibit an open-cell structure, the location of the specimen during test has a significant influence on the strength but not the modulus.

ACKNOWLEDGMENTS

This work was supported by major Special Project of Guizhou (Grant no. 6023), Science and technology plan projects of Guiyang (Grant no. [2012101HK] 209-16), and NNSF of China (201264004).

REFERENCES

1. Komai, K.; Minoshima, K.; Tanaka, K.; Tokura, T. *Int. J. Fatigue* **2002**, *24*, 339.
2. Alonso, M. V.; Auad, M. L.; Nutt, S. *Compos. A* **2006**, *37*, 1952.
3. Karthikeyan, C. S.; Sankaran, S.; Kishore. *Mater. Lett.* **2004**, *58*, 995.
4. Gupta, N.; Woldesenbet, E. *J. Compos. Mater.* **2005**, *39*, 2197.
5. Tagliavia, G.; Porfiri, M.; Gupta, N. *Compos. B Eng.* **2010**, *41*, 86.
6. Asif, A.; Rao, L. V.; Ninan, K. N. *Mater. Sci. Eng. A* **2010**, *527*, 6184.
7. Tagliavia, G.; Porifiri, M.; Gupta, N. *Compos. B* **2012**, *43*, 115.
8. Mcelhanon, J. R.; Russick, E. M.; Wheeler, D. R.; Loy, D. A.; Aubert, J. H. *J. Appl. Polym. Sci.* **2002**, *85*, 1496.
9. Zhong, F.; He, J.; Wang, X. *J. Appl. Polym. Sci.* **2009**, *112*, 3543.
10. Kiefer, J.; Hilborn, J. G.; Månson, J. A. E.; Leterrier, Y. *Macromolecules* **1996**, *29*, 4158.
11. Stefani, P. M.; Tejeira, B. A.; Sabugal, J.; Vazguez, A. *J. Appl. Polym. Sci.* **2003**, *90*, 2992.
12. Wan Hamad, W. N. F.; The, P. L.; Yeoh, C. K. *Polym. Plast. Technol. Eng.* **2013**, *52*, 754.
13. Takiguchi, O.; Ishikawa, D.; Sugimoto, M. *J. Appl. Polym. Sci.* **2008**, *110*, 657.
14. Chen, K.; Tian, C.; Lu, A.; Zhou, Q.; Jia, X.; Wang, J. *J. Appl. Polym. Sci.* **2014**, *131*.
15. Wang, M.; Cilliers, J. *J. Chem. Eng. Sci.* **1999**, *54*, 707.
16. Swetha, C.; Kumar, R. *Mater. Des.* **2011**, *32*, 4152.
17. Mae, H. *Mater. Sci. Eng. A* **2008**, *496*, 455.
18. Barzegari, M. R.; Rodrigue, D. *Polym. Eng. Sci.* **2007**, *47*, 1459.
19. Chen, Z.; Yan, N.; Sam-Brew, S.; Smith, G.; Deng, J. *Eur. J. Wood Wood Product.* **2014**, 1.
20. Johnson, A. F.; Sims, G. D. *Composites* **1986**, *17*, 321.
21. Xing, Z.; Wu, G. Z.; Huang, S. R. *J. Supercrit. Fluids* **2008**, *47*, 281.
22. Matuana, L. M.; Faruk, O.; Diaz, C. A. *Bioresour. Technol.* **2009**, *100*, 5947.
23. Najib, N. N.; Ariff, Z. M.; Bakar, A. A.; Sipaut, C. S. *Mater. Des.* **2011**, *32*, 505.
24. Tai, H. J. *J. Polym. Res.* **2005**, *12*, 457.
25. Zhang, X.; Wang, J.; Fan, Z. *J. Aeronaut. Mater.* **2003**, *23*, 186.
26. Alonso, M. V.; Auad, M. L.; Nutt, S. R. *Composit. Sci. Technol.* **2006**, *66*, 2126.
27. Wang, L.; Zhang, J.; Yang, X.; Zhang, C.; Gong, W.; Yu, J. *Mater. Des.* **2014**, *55*, 928.
28. Karthikeyan, C. S.; Sankaran, S.; Kishore. *Polym. Adv. Technol.* **2007**, *18*, 254.
29. Wouterson, E. M., Boey, F. Y. C.; Hu, X.; Wong, S. C. *Composit. Sci. Technol.* **2007**, *11–12*, 1840.